ACS Catalysis

Research Article

pubs.acs.org/acscatalysis

Engineering and Sizing Nanoreactors To Confine Metal Complexes for Enhanced Catalytic Performance

Mozaffar Shakeri,[†] Lucian Roiban,[†] Vital Yazerski,[‡] Gonzalo Prieto,[†] Robertus J. M. Klein Gebbink,[‡] Petra E. de Jongh,[†] and Krijn P. de Jong*[,†]

[†]Inorganic Chemistry and Catalysis, Debye Institute for Nanomaterials Science and [‡]Organic Chemistry and Catalysis, Debye Institute for Nanomaterials Science, Utrecht University, Universiteitsweg 99, 3584 CG Utrecht, The Netherlands

Supporting Information

ABSTRACT: Homogeneous metal complexes often display superior activity and selectivity in catalysis of chemical transformations. Heterogenization of these complexes by immobilization on solid supports has been used to facilitate recovery, but this is often associated with a decrease in catalytic performance. We here describe a novel approach of sizing and engineering the cavity structure of nanoporous materials as "nanoreactors" to assemble metal complexes by the "ship-in-the-bottle" synthesis to combine the best of homogeneous and heterogeneous catalysts. Catalysis occurred by free metal complexes in confined liquid in these nanoreactors, while the catalysts were recyclable as being heterogeneous at the macroscopic scale. Subnanometer tailoring of window sizes (0.5−3.7 nm) of the cavities (16−22 nm) allowed control over loading (6−70 mg-metal complex/g-support) and a high turnover frequency (40−600 h^{-1}) for the hydrolytic kinetic resolution of 1,2-epoxyhexane. Most importantly, the 'heterogeneous homogeneous catalysts' showed enhanced thermal stability and were stable upon reuse approaching excellent turnover numbers of 100,000. We showed that engineering and sizing of nanoreactors is a powerful approach to control performance of confined catalysts, and this method is generally applicable in host−guest catalysis.

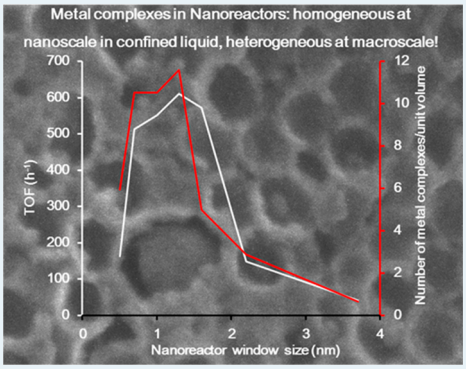

KEYWORDS: *mesocellular foam, metal salen complexes, ship in the bottle synthesis, heterogeneous catalysis, sizing nanoreactor*

INTRODUCTION

Catalysis is the key technology for production of transportation fuels as well as in the petrochemical, commodity and fine chemicals, and pharmaceutical industries. Heterogeneous catalysts exhibit facile separation from products and high stability even at elevated temperatures.[1] Homogeneous metal complexes show higher activity and selectivity with the possibility of fine-tuning by subtle change of their structure. The metal complexes however do not tolerate high temperatures and often have limited productivity, and their separation and reuse is a serious challenge for large scale industrial applications. Anchoring of metal complexes on solid supports by various methods, with covalent immobilization as the most widely used, has been investigated in both academia and industry to facilitate recovery, but this often deteriorates the performance of the catalysts. Solid catalysts that combine the best of the worlds of homogeneous and heterogeneous catalysis are highly desired but have remained elusive even after 40 years of intense research.[2]

An important development has been the so-called "ship-in-the-bottle"(SIB) synthesis. Using microporous solids, in particular zeolites, by infiltration of precursors metal complexes were built up inside the pores, but these systems showed limited activity by spatial restrictions of the metal complexes in the small cavities (≈1.0 nm).[3−6] Nanoporous materials with bigger and tunable cavities "nanoreactors", synthesized by amphiphilic triblock copolymer templates, show larger potential in this respect.[7−11] For example, the Li group has studied [Co(salen)] complexes in nanoporous materials of SBA-16 and FDU-12 and obtained enhanced activities by realizing high metal complex concentrations.[12−14] These types of metal complexes obey second order kinetic reaction dependency on the catalyst concentrations by using bimetallic centers to coordinate the substrates and catalyze many important reactions (Supplementary Figure S1).[15−20]

Despite the progress made in the heterogenization of metal complexes in nanoporous supports, only a few have been commercialized.[21] This mainly arises from challenges in control and assessment of nanocavity sizes and accessibility sizes of the support materials related to catalysts performance which lead to problems with (*i*) activity and substrates scope, (*ii*) catalyst loading, (*iii*) reproducibility, and (*iv*) productivity. We recently investigated tailoring window sizes of plugged nanochannels of SBA-15 materials and confine metal complexes to control activity.[22,23] The obtained catalysts showed enhanced activity but limited substrate scope and low productivity and retained

Received: June 6, 2014
Revised: September 9, 2014
Published: September 10, 2014

   dx.doi.org/10.1021/cs500777q | *ACS Catal.* 2014, 4, 3791−3796

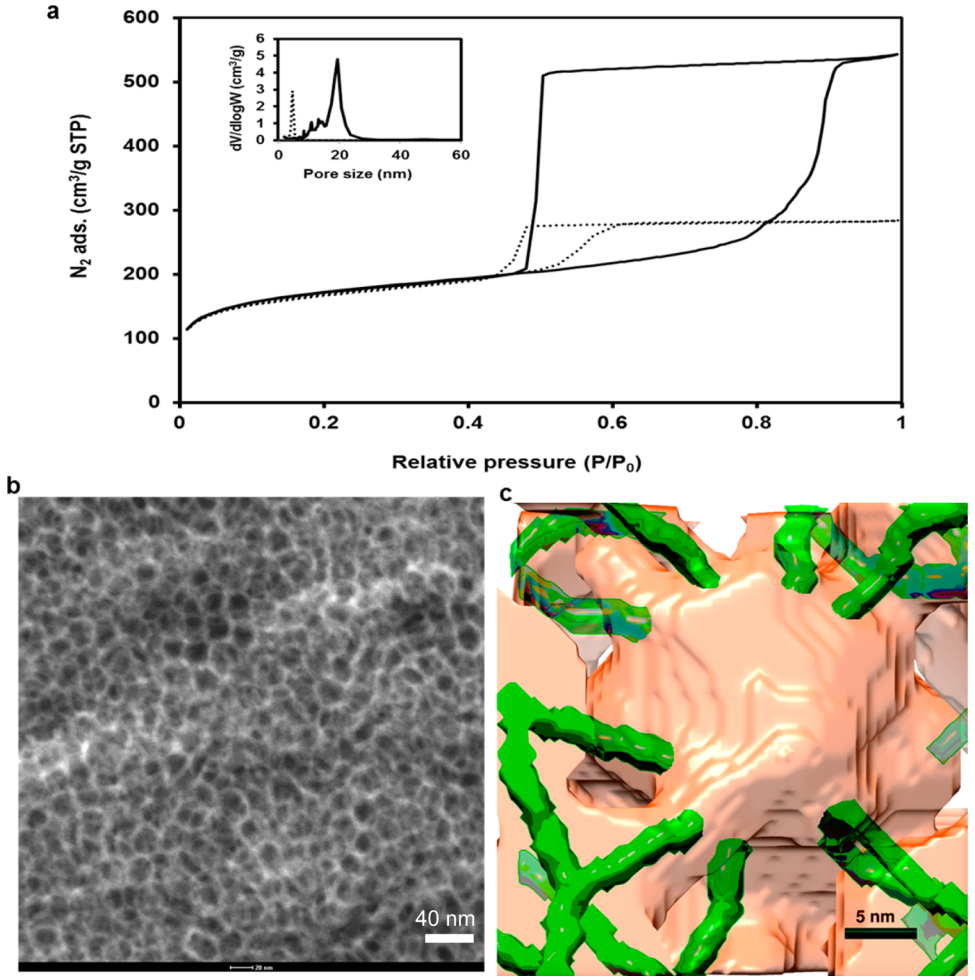

Figure 1. N_2 isotherms and electron microscopy analysis of m-MCF materials. (**a**) N_2 isotherms and pore size distributions (insert) of m-MCF-3 (full line) and an original plugged SBA-15 (dotted line) which were synthesized at 70 °C, (**b**) STEM-HAADF images of m-MCF-3, and (**c**) an electron tomography model of a single cavity (orange) of m-MCF-6 connected with 9 neighboring pores (green).

low amounts of metal complexes.[24] Control of accessibility (size and number of windows) and nanocavity sizes of the host materials are expected to be beneficial to make robust heterogeneous catalysts with metal complexes in the confined liquid in nanocavities.

Engineering of nanochannels of SBA-15 has resulted previously in mesocellular foam (MCF) materials with better porosity with (3D) cage-like pores of 20−40 nm and window sizes 10−20 nm.[25−27] These materials were promising to host metal nanocatalysts[28,29] and metal complexes through chemical grafting due to fast mass transfer.[30−32] However, they are not suitable to host metal complexes in confined liquid due to windows much bigger relative to the guest sizes. In this article we report on the synthesis, control, and assessment of a new class of MCF materials referred to as "modified MCF" (m-MCF) suitable to host metal complexes. We describe tailoring of cage sizes of 16−22 nm in diameter, window sizes of 1.8−5.0 nm, and wall thicknesses of 4−7 nm of nanoreactors of m-MCFs by manipulating the synthesis conditions, in particular the hydrothermal treatment temperatures, and by addition of a swelling agent to enhance the performance of confined metal complexes. We show that the m-MCFs thus prepared are powerful to control assembly and catalytic performance of [Co(salen)] complexes.

RESULTS AND DISCUSSION

Synthesis and Characterization of m-MCFs. We first investigated control of the pore dimensions of plugged SBA-15 materials by the use of trimethylbenzene as a swelling agent at different hydrothermal treatment temperatures. This resulted in materials with combined and controlled structural properties of MCF and plugged SBA-15 which is referred to as modified mesocellular foam "m-MCF". N_2 isotherms of m-MCFs showed much higher adsorption and broader hysteresis compared to plugged SBA-15 indicating higher porosity (Figure 1a and Supplementary Figure S2). Capillary condensation of N_2 in m-MCFs similarly to conventional MCF occurred at a high relative pressure of 0.85−0.90 which indicates formation of the large pore size materials (Figure 1a and Supplementary Figure S2 and Figure S3). The mean pore sizes of m-MCFs, obtained from N_2 adsorption branches, increased from 16 to 22 nm upon hydrothermal treatment at increasing temperatures (Table 1 and Supplementary Figure S2).

N_2 desorption of conventional MCF occurred at a relative pressure of 0.86, and thus the window size (15.0 nm) was obtained from the desorption isotherm (Supplementary Figure S3).[25] However, desorption from m-MCFs was delayed toward a low relative pressure of about 0.49, similarly to plugged SBA-15, which is an indication for "ink-bottle" type pores consisting of large cavities connected by small windows ≤5 nm (Figure 1a

dx.doi.org/10.1021/cs500777q | ACS Catal. 2014, 4, 3791−3796

Table 1. Structural Properties of m-MCFs and Related Materials

entry	material[a]	temp (°C)	S_{BET}[b] (m^2/g)	PV[c] (cm^3/g)	V_{micro}[d] (cm^3/g)	PD[e] (nm)	W[f] (nm)
1	m-MCF-1	50	450	0.59	0.09	16	1.8
2	m-MCF-2	60	540	0.73	0.12	17	2.0
3	m-MCF-3	70	580	0.83	0.08	19	2.3
4	m-MCF-4	80	790	1.0	0.14	18	2.9
5	m-MCF-5	90	570	0.94	0.06	19	3.5
6	m-MCF-6	100	670	1.2	0.07	22	5.0
7[g]	plugged SBA-15	70	570	0.44	0.12	5.0	2.3
8	MCF	100	580	2.2	0.02	28	15[h]

[a]m-MCF-x materials synthesized at different temperatures. [b]S_{BET}, BET surface area. [c]PV, pore volume. [d]V_{micro}, micropore volume. [e]PD, pore diameter. [f]W, window size calculated by surface functionalization with akoxysilanes. [g]Data were taken from ref 23. [h]Window size obtained from N_2 desorption isotherm.

and Supplementary Figure S2). Since liquid N_2 is unstable below about 0.49, calculation of window sizes from desorption branches is not possible.[33−36] Surfaces of m-MCFs thus were functionalized with various alkoxysilanes, and window sizes were calculated from the length of shortest alkyl group which blocked N_2 adsorption (Table 1).[23,37,38] The results show that the window size increases with hydrothermal treatment temperature. The increase is 0.2−0.3 nm/10 °C giving window sizes in the range of 1.8−2.9 nm for hydrothermal treatment temperatures of 50−80 °C. However, a larger dependency (0.5−1.5 nm/10 °C) was observed at temperatures above 80 °C, resulting in window sizes of 3.5−5.0 nm. This might originate from dehydration of the hydrophobic core and more trimethylbenzene accumulation at the hydrophilic corona resulting in a phase change of the micelles at increased temperature.[26]

An electron microscopy study was conducted to gain insight in the pore structure and morphology of the m-MCFs.[39,40] STEM-HAADF indicated cavities with spherical structure (Figure 1b), while electron tomography analysis demonstrated that each spherical cavity of m-MCF-6 is connected to 9−12 neighboring cavities resulting in a highly interconnected network with windows of 4−5 nm in agreement with data from surface functionalization (Figure 1c and Supplementary Figure S4). SEM showed that m-MCFs consist of spherical-particles of 2−3 μm diameter (Supplementary Figure S5). Overall, characterization demonstrated that the obtained m-MCFs possess excellent connectivity, large cavities, and small-and-well tailored windows which might be eminently suitable for host−guest catalysis. We therefore grafted m-MCFs and an MCF with alkyl groups and used them to host [Co(salen)] complexes through the SIB synthesis (For structural properties of alkyl grafted m-MCFs, designated as m-MCF-C_n, see Supplementary Table S1.).

Control of Loading, Local Concentration, and Activity of [Co(salen)] in m-MCFs. The amount of metal complexes in nanoporous support is crucial to control performance of catalysts and for their large scale applications. This will be influenced by pore dimensions such as cavity and window sizes. Loading of [Co(salen)] in various m-MCFs-C_3 showed strong dependency on the window sizes probably as a result of diffusion resistance during synthesis and leaching of metal complexes during washing (Figure 2a). Loading of [Co(salen)] in m-MCFs-C_3 increased upon increase of the window sizes, reached a maximum of about 73 mg/g-support at window sizes of 1.0−1.3 nm, and then sharply decreased upon further increase of the window sizes. m-MCFs-C_3 with window sizes ≤0.7 nm contained a lower amount of [Co(salen)] possibly due to mass transfer resistance during the SIB synthesis. m-MCFs-C_3 with window sizes ≥1.6 nm showed lower loading because bigger window sizes brought less retaining power during washing. Loading of [Co(salen)] in m-MCFs-C_3 with window sizes of 2.2 and 3.7 nm decreased to 21 and 5.6 mg/g-support (Figure 2a), respectively, and it was virtually nil for conventional MCF-C_3 with window size of 14 nm (Supplementary Table S1).

The weight loading of [Co(salen)] in m-MCFs-C_3 is about 2- to 5-fold higher than that in plugged SBA-15-C_3 materials for similar window sizes (Figure 2a). For example, m-MCF-C_3 with window size of 1.0 nm and 2-fold higher total pore volume retained 5-fold more [Co(salen)] than that by plugged SBA-15-C_3. This is possibly contributed by the larger cavity sizes and by

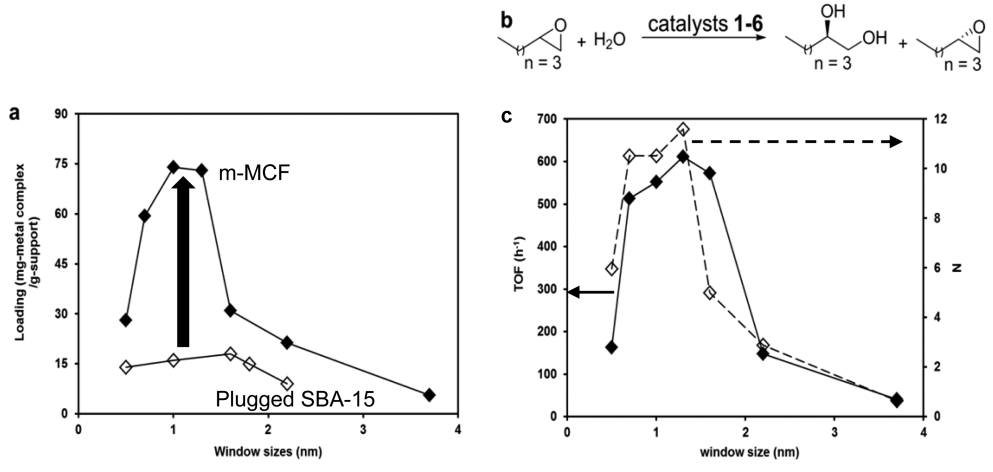

Figure 2. Trend of loading and catalytic performance of [Co(salen)] in m-MCFs. (**a**) Trend of [Co(salen)] loading of catalyst **1**−**6** in m-MCFs-C_3 (◆) and that in plugged SBA-15-C_3 materials with window sizes (◊) of ref 24 and (**b**) HKR of 1,2-epoxyhexane by catalysts **1**−**6**, (**c**) turnover frequency (TOF) (◆) and local concentration, *N* (average number of metal complexes/100 nm^3 of pore volume) (◊) vs window sizes for catalysts **1**−**6**. m-MCF with window size of 1.3 nm was grafted with ethyl groups (m-MCF-C_2) and the obtained catalyst is named catalyst **3b**.

dx.doi.org/10.1021/cs500777q | ACS Catal. 2014, 4, 3791−3796

improved accessibility, i.e., 9−12 windows per cavity of m-MCF compared to 2 windows per nanochannel of SBA-15.

We then compared the SIB synthesis with pore filling of the final complex in nanoporous materials. The pore filling of a conventional MCF-C_3 by [Co(salen)] resulted in no loading as a result of leaching during washing (Supplementary Table S1, catalyst **8**). A similar approach with an m-MCF-C_3 also resulted in no loading; however, this was caused by limitation of [Co(salen)] diffusion into the cavities as the SIB synthesis showed a significant loading as mentioned earlier (Supplementary Table S1; catalysts **6** and **9**). These results suggest that SIB synthesis with tailoring nanoporous materials is a superior approach to arrive at a high amount of metal complexes inside the cavities.

The activity of [Co(salen)] in nanoporous materials was strongly affected by local concentration of metal complexes, *N* (average number of metal complexes/100 nm^3 of pore volume) as well as window size.[24] We therefore investigated control of activity of catalysts **1**−**6** relative to pore accessibility and local catalyst concentration in HKR of 1,2-epoxyhexane (Figure 2b). The local concentration of [Co(salen)] in m-MCFs-C_3, *N* (average number of metal complexes/100 nm^3 of pore volume) changed with window size for catalysts **1**−**6** (Figure 2c). The *N* was 6 for a window size of 0.5 nm, increased to 10.5 and 11.6 for window sizes of 0.7 and 1.3 nm, and then decreased to 5 for a window size of 1.6 nm and to 2.9 for a window size of 2.2 nm. The *N* was only 0.65 for window size of 3.7 nm. Turnover frequencies (TOF) of the obtained catalysts **1**−**6** in HKR of 1,2-epoxyhexane followed three regimes depending on the *N* and window sizes, while all showed excellent enantioselectivity of ee >99% for 1,2-hexanediol (for kinetics of the reactions see Supplementary Figure S6). For window sizes ≤0.7 nm the activity was increased by increase in size possibly as a result of faster mass transfer and binuclear complex activation at $N \geq 5$.[24] For window sizes of 0.7−1.6 nm and *N* of 5−11.6 the activity varied little as a result of the absence of mass transfer limitation and sufficient binuclear activation. For window sizes of 2.2 and 3.7 nm with *N* of 2.9 and 0.65 the activity decreased sharply showing that *N* was not high enough to fully satisfy binuclear activation of the substrates. Thus, it is concluded that for $N \geq 5$ and fast mass transfer the highest activity resulted.

We furthermore compared the activity of [Co(salen)] in m-MCF-C_3 and that in plugged SBA-15-C_3. The results showed that e.g., catalyst **4** in this study was much more active than [Co(salen)] in plugged SBA-15-C_3 for similar window size, *N*, and reactions conditions (Supplementary Figure S7). This possibly arises from faster mass transfer due to the higher number of windows per cavity for m-MCFs.

A limited substrate scope is another serious challenge of confined catalysts in cavities present in zeolites. We therefore compared the HKR activity of our catalysts with others for more challenging substrates of styrene oxides and 1,2-epoxydecane (Supplementary Table S2). The results showed higher activity with excellent enatioselectivity of obtained 1,2-diols for our catalysts, indicating that engineering nanoporous materials is a powerful approach to enhance catalytic performance of homogeneous metal complexes.

Thermal Stability of [Co(salen)] in m-MCFs. Thermostable homogeneous catalysts are prerequisite to enhance reaction rates and to extend reaction scope.[41] However, this is often hindered by limited stability and selectivity of the metal complexes at higher temperatures. The HKR of 1,2-epoxyhexane thus at various temperatures using catalyst **2** and the related homogeneous catalyst were conducted (Figure 3).

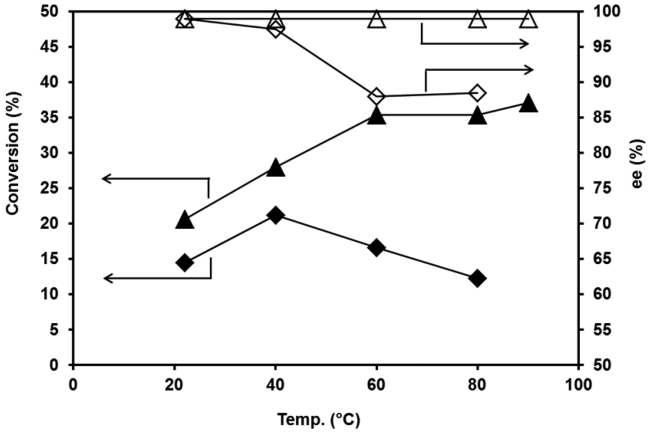

Figure 3. Thermostability of confined and homogeneous catalysts. Conversion (%) (closed symbols) and enantioselectivity (open symbols) of catalyst **2** (triangles) after 1 h and homogeneous [Co(salen)] (diamonds) after 48 h in the HKR of 1,2-epoxyhexane at various temperatures. The Co loadings relative to substrate were 0.05 mol % for catalyst **2** and 0.1 mol % for the homogeneous catalyst.

Conversion increased upon increase in temperature and leveled off at about 80 °C reaching 35% conversion in 1 h by catalyst **2**, while that by the homogeneous catalyst reached a maximum of 21% conversion in 48 h at 40 °C and then decreased upon increase in temperature. Catalyst **2** showed high enantioselectivity (99%) for 1,2-hexanediol even at a temperature of 90 °C, while the enantioselectivity of the homogeneous catalyst decreased to 88% at 60 °C (Figure 3). Catalyst **2** maintained its activity over the reaction time; however, the homogeneous catalyst was active over 2 h and then largely lost its activity (Supplementary Figure S8). This might originate from faster substitution of acetate with water at higher temperatures which initially results in appreciable activity, but a higher proportion of Co−OH species over time may lead to deactivation of the homogeneous catalyst (Supplementary Figure S1). Catalyst **2** however was possibly protected from fast acetate substitution by the hydrophobic nature of the support material and this led to sustained activity over time. These results demonstrate the potential of confinement to make thermostable metal complex catalysts to enhance reaction rates and extend reactions scope.

Recyclability and Productivity Assessment of [Co(salen)] in m-MCFs. Catalyst **3b** was recycled for six cycles of HKR of 1,2-epoxyhexane with preserved activity and enantioselectivity, while a reactivation process between the cycles was *not* conducted (Supplementary Figure S9). Initially catalyst **3b** was recycled for four cycles at catalyst loading of 0.067 mol % where each batch was done in 2 h with ee >99% for 1,2-hexanediol. These conditions lead to a TON of 670 mol. product/mol. Co for each batch. Catalyst **3b** after recovery was subsequently supplied with ten times more substrate (catalyst loading of 0.0067 mol %), and a conversion of 44% was achieved in 20 h then followed by another batch (0.067 mol %) with almost unaffected activity and enantioselectivity. Encapsulated [Co(salen)] in shell cross-linked micelle-based nanoreactors, however, lost almost 50% of its initial activity after 6 runs when the catalyst was not reactivated among the cycles.[42] These results encouraged us to run the HKR in extremely low

dx.doi.org/10.1021/cs500777q | *ACS Catal.* 2014, 4, 3791−3796

catalyst loading (3.35×10^{-4} mol %) but still high local catalyst concentration to arrive 25.6% conversion at a total turnover number of 76,000 (mol. product/mol. Co catalyst) which is a factor of 5 or more higher than any of those reported so far (Figure 4)[24,42−44] and is equal to that which could be obtained

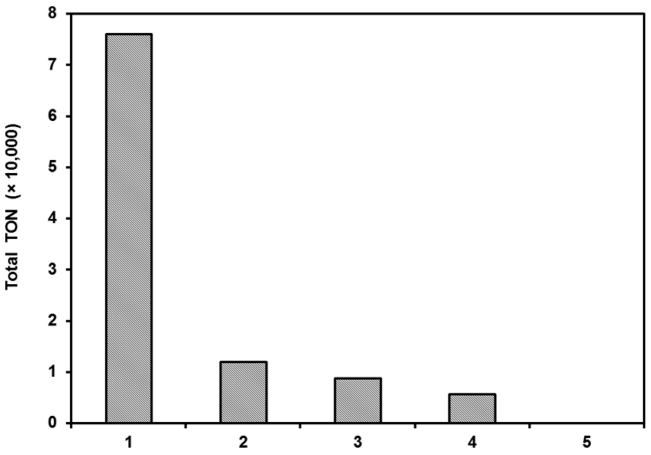

Figure 4. Productivity assessment of catalyst **3b**. Total TON (mol. product/mol. Co catalyst): entry 1 (catalyst **3b** in this study), entry 2 (ref 24), entry 3 (ref 42), entry 4 (ref 43), and entry 5 (ref 44).

by about 110 small batches (76,000/670 ≈ 110). This achievement suggests that engineering nanoporous materials is a powerful approach to control activity and selectivity as well as stability and to combine the best of homogeneous and heterogeneous catalysts to meet industrial needs.

CONCLUSION

A new class of mesocellular foams (MCF) materials, designated as m-MCFs, was synthesized with control over the pore and window sizes for the purpose of host−guest applications. We showed that sizing nanoporous materials is a powerful approach to enhance the performance of metal complexes in confined liquids in nanoreactors obtained through the SIB synthesis. A strong dependency of the activity on local catalyst concentration and the window sizes was found. We showed that the [Co(salen)]/m-MCFs catalysts were more active and stable over a wider range of temperatures than the corresponding free homogeneous catalyst and others reported previously. The high loading and activity of metal complexes in m-MCFs compared to that in other nanoporous materials might originate mainly from the larger spherical cavity and more numerous connectivity. The obtained catalysts could be recycled *without* reactivation among the cycles and resulted in the highest TON values of 76,000 reported thus far for the HKR. We showed that engineering and sizing of nanoporous materials results in catalysts with the best of both homogeneous and heterogeneous catalysis. This approach is generally applicable in host−guest catalysis and would be highly beneficial to control performance of confined catalysts in nanoporous materials. Our laboratory currently is investigating this approach for other catalysts.

METHODS

Materials. All materials were used as received from the suppliers without further purification.

Synthesis and Functionalization of Conventional and Modified MCF Materials. MCF with large window sizes (conventional MCF) was synthesized based on a reported procedure.[27] Synthesis and functionalization of modified MCF materials (m-MCFs) with small window sizes (≤5 nm) were conducted based on an adapted procedure for plugged SBA-15 as described below.[23] Four grams of copolymer Pluronic P123 (poly(ethylene oxide)-*block*-poly(propylene oxide)-*block*-poly-(ethylene oxide), $EO_{20}PO_{70}EO_{20}$, M_{av} = 5800) was dissolved in an aqueous acidic solution (150 mL; 1.6 M) in a 500-mL polypropylene bottle at room temperature over a night. 1,3,5-Trimethylbenzene (TMB; 3 g) was added to the reaction mixture at 30 °C, stirred for 2 h, followed by slow addition of TEOS (17 g) at 35 °C in 12 min and further stirring for another 5 min. The reaction mixture was aged at 39 °C for 20 h followed by hydrothermal treatment at a temperature of 50, 60, 70, 80, 90, or 100 °C for 1 d. The m-MCFs then were washed with water, dried, and calcined at 550 °C for 6 h.

Characterization of Conventional MCF and m-MCF Materials. m-MCFs were characterized by N_2 physisorption, scanning electron microscopy (SEM), transmission electron microscopy (TEM), scanning transmission electron microscopy high-annular angle dark field (STEM-HAADF), and electron tomography (ET).[39,40] N_2 physisorption were conducted to determine pore size, pore and micropore volumes, and BET surface area (Supporting Information). To determine the window sizes, each m-MCF was functionalized with different alkoxysilanes and subjected to N_2 physisorption. The window sizes were calculated from the shortest alkyl chain blocking N_2 adsorption by the formula of window size [nm] = 0.75 + 2 × (*n*-1) × 0.125 [nm] where *n* is the number of carbon chain (Table 1).[23,37,38]

Electron microscopy analysis by STEM-HAADF, ET, and SEM were conducted on an m-MCF sample to get insight in pore geometry, connectivity and particles morphology (details in the Supporting Information).

Ship in the Bottle (SIB) Synthesis of [Co(salen)] in m-MCFs. The SIB synthesis of (*S*,*S*)-(+)-*N*,*N*-bis(3,5-di-*tert*-butylsalicylidene)-1,2-cyclohexanediamino cobalt(III)acetate ([Co(salen)]) in m-MCFs and a conventional MCF were conducted similarly to those in plugged SBA-15 as described below (Figure S10).[24] Six m-MCFs and a conventional MCF were first functionalized by *n*-propyltriethoxysilane to passivate the silanol groups (structural properties in Supplementary Table S1 and Supplementary Figure S11). Furthermore, an m-MCF sample was functionalized with ethyltriethoxysilane (m-MCF-C_2). The SIB synthesis in m-MCFs-C_3, an m-MCF-C_2, and a conventional MCF-C_3 were conducted by diffusing precursors one by one under mild reaction conditions and oxidation of the [Co(II) (salen)] to [Co(III)(salen)] ([Co-(salen)] onward in this study) by acetic acid in toluene (1:9) under air. The resulting catalysts, named catalysts **1**−**6** (Table S1), were washed with toluene, methanol, and DCM and dried under vacuum and characterized by N_2 physisorption (Supplementary Figure S11 and Table S1), FT-IR (Supplementary Figure S12), and UV−vis (Supplementary Figure S13).

The pore filling of [Co(salen)] in an m-MCF-C_3 and an MCF-C_3 were conducted to compare it with the SIB results. Sixty mg of [Co(salen)] was added to half a gram of an m-MCF-C_3 or a conventional MCF-C_3 in methanol (3 mL) and stirred for 48 h. The resulting catalysts then were washed with toluene, methanol, and DCM and dried under vacuum (Supplementary Table S1).

dx.doi.org/10.1021/cs500777q | *ACS Catal.* 2014, 4, 3791−3796

Hydrolytic Kinetic Resolution (HKR) of Terminal Epoxides. HKR of terminal epoxides were conducted by addition of a substrate to heterogeneous [Co(salen)] or free homogeneous [Co(salen)] (X mol % of [Co(salen)] relative to the terminal epoxide) in a 20 mL screw cap vial followed by addition of H_2O (0.75 eq. related to the terminal epoxide) at 0 °C. The reaction mixture was then allowed to reach room temperature or put directly in the oil bath at the desired temperature and stirred, and samples were taken intermittently to check the conversion ratios (%) and enantiomeric excess (ee) of obtained 1,2-diols (Supporting Information).

Thermal stability study of obtained catalysts, [Co(salen)]/m-MCF-C_3 and homogeneous [Co(salen)], was conducted by HKR of 1,2-epoxyhexane at different temperatures of 40, 60, 80, and 90 °C. The Co loadings relative to substrate were 0.05 mol % and 0.1 mol % for catalyst **2** and homogeneous [Co(salen)], respectively.

For productivity assessment of obtained catalysts, HKR of 1,2-epoxyhexane was conducted in 3.35×10^{-4} mol % of catalyst **3b**. The total turnover number (TON) was calculated based on total moles of 1,2-epoxyhexane transformed by one mole of confined [Co(salen)] in m-MCF-C_2.

■ ASSOCIATED CONTENT

Supporting Information

Details of N_2 physisorption of m-MCFs and alkyl-grafted m-MCFs; SEM images of m-MCFs and plugged SBA-15; ET results of an m-MCF; details of HKR reaction by the catalysts **1**−**6**; FT-IR, UV−vis, and physical properties of the catalysts **1**−**6**. This material is available free of charge via the Internet at http://pubs.acs.org.

■ AUTHOR INFORMATION

Corresponding Author

*E-mail: k.p.dejong@uu.nl.

Notes

The authors declare no competing financial interest.

■ ACKNOWLEDGMENTS

This work is supported financially by the Dutch National Research School Combination Catalysis (NRSCC). Support from NWO-TOP (KPdJ) and NWO-VICI (PEdJ) is also acknowledged. The TEM and UV−vis studies were done by Hans Meeldijk and Qingyun Qian.

■ REFERENCES

(1) Torres Galvis, H. M.; Bitter, H. J.; Khare, B. C.; Ruitenbeek, M.; Dugulan, A. I.; de Jong, K. P. *Science* **2012**, *335*, 835−838.
(2) Rothenberg, G. *Nat. Chem.* **2010**, *2*, 9−10.
(3) Herron, N. *Inorg. Chem.* **1986**, *25*, 4714−4717.
(4) Sabater, M. J.; Corma, A.; Domenech, A.; Fornes, V.; Garcia, H. *Chem. Commun.* **1997**, 1285−1286.
(5) Ogunwumi, S. B.; Bein, T. *Chem. Commun.* **1997**, 901−902.
(6) Corma, A.; Gracia, H. *Eur. J. Inorg. Chem.* **2004**, 1143−1164.
(7) Zhao, D.; Huo, Q.; Feng, J.; Chmelka, B. F.; Stucky, G. D. *J. Am. Chem. Soc.* **1998**, *120*, 6024−6036.
(8) Liu, X.; Tian, B.; Yu, C.; Gao, F.; Xie, S.; Tu, B.; Che, R.; Peng, L.-M.; Zhao, D. *Angew. Chem., Int. Ed.* **2002**, *41*, 3876−3878.
(9) Fan, J.; Yu, C.; Gao, F.; Lei, J.; Tian, B.; Wang, L.; Luo, Q.; Tu, B.; Zhou, W.; Zhao, D. *Angew. Chem., Int. Ed.* **2003**, *42*, 3146−3150.
(10) Kleitz, F.; Liu, D. N.; Anilkumar, G. M.; Park, I. S.; Solovyov, L. A.; Shmakov, A. N.; Ryoo, R. *J. Phys. Chem. B* **2003**, *107*, 14296−14300.
(11) Chng, L. L.; Erathodiyil, N.; Ying, J. Y. *Acc. Chem. Res.* **2013**, *46*, 1825−1837.
(12) Yang, H.; Zhang, L.; Zhong, L.; Yang, Q.; Li, C. *Angew. Chem., Int. Ed.* **2007**, *46*, 6861−6865.
(13) Li, B.; Bai, S.; Wang, X.; Zhong, M.; Yang, Q.; Li, C. *Angew. Chem., Int. Ed.* **2012**, *51*, 11517−11521.
(14) Yang, H.; Zhang, L.; Su, W.; Yang, Q.; Li, C. *J. Catal.* **2007**, *248*, 204−212.
(15) Konsler, R. G.; Karl, J.; Jacobsen, E. N. *J. Am. Chem. Soc.* **1998**, *120*, 10780−10781.
(16) Annis, D. A.; Jacobsen, E. N. *J. Am. Chem. Soc.* **1999**, *121*, 4147−4154.
(17) Schaus, S. E.; Brandes, B. D.; Larrow, J. F.; Tokunaga, M.; Hansen, K. B.; Gould, A. E.; Furrow, M. E.; Jacobsen, E. N. *J. Am. Chem. Soc.* **2002**, *124*, 1307−1315.
(18) Nielsen, L. P. C.; Stevenson, C. P.; Blackmond, D. G.; Jacobsen, E. N. *J. Am. Chem. Soc.* **2004**, *126*, 1360−1362.
(19) Nielsen, L. P. C.; Zuend, S. J.; Ford, D. D.; Jacobsen, E. N. *J. Org. Chem.* **2012**, *77*, 2486−2495.
(20) Gill, C. S.; Venkatasubbaiah, K.; Phan, N. T. S.; Weck, M.; Jones, C. W. *Chem.—Eur. J.* **2008**, *14*, 7306−7313.
(21) Jones, C. W. *Top Catal.* **2010**, *53*, 942−952.
(22) van der Voort, P.; Ravikovitch, I.; de Jong, K. P.; Benjelloun, M.; van Bavel, E.; Janssen, A. H.; Neimark, A. V.; Weckhuysen, B. M.; Vansant, E. F. *J. Phys. Chem. B* **2002**, *106*, 5873−5877.
(23) Shakeri, M.; Klein Gebbink, R. J. M.; de Jongh, P. E.; de Jong, K. P. *Microporous Mesoporous Mater.* **2013**, *170*, 340−345.
(24) Shakeri, M.; Klein Gebbink, R. J. M.; de Jongh, P. E.; de Jong, K. P. *Angew. Chem., Int. Ed.* **2013**, *52*, 10854−10857.
(25) Schmidt-Winkel, P.; Lukens, W. W., Jr.; Zhao, D.; Yang, P.; Chmelka, B. F.; Stucky, G. D. *J. Am. Chem. Soc.* **1999**, *121*, 254−255.
(26) Schmidt-Winkel, P.; Glinka, C. J.; Stucky, G. D. *Langmuir* **2000**, *16*, 356−361.
(27) Han, Y.; Lee, S. S.; Jing, J. Y. *Chem. Mater.* **2006**, *18*, 643−649.
(28) Tsung, C.-K.; Kuhn, J. N.; Huang, W.; Aliaga, C.; Hung, L.-I.; Somorjai, G. A.; Yang, P. *J. Am. Chem. Soc.* **2009**, *131*, 5816−5822.
(29) Prieto, G.; Zecevic, J.; Friedrich, H.; de Jong, K. P.; de Jongh, P. E. *Nat. Mater.* **2013**, *121*, 34−39.
(30) Huang, X.; Jing, J. Y. *Chem. Commun.* **2007**, 1825−1827.
(31) Lim, J.; Riduan, S. N.; Lee, S. S.; Ying, J. Y. *Adv. Synth. Catal.* **2008**, *350*, 1295−1308.
(32) Jee, J.-E.; Cheong, J. L.; Lim, J.; Chen, C.; Hong, S. H.; Lee, S. S. *J. Org. Chem.* **2013**, *78*, 3048−3056.
(33) Ravikovitch, P. I.; Neimark, A. V. *Langmuir* **2002**, *18*, 1550−1560.
(34) Ravikovitch, P. I.; Neimark, A. V. *Langmuir* **2002**, *18*, 9830−9837.
(35) Rasmussen, C. J.; Vishnyakov, A.; Thommes, M.; Smarsly, B. M.; Kleitz, F.; Neimark, A. V. *Langmuir* **2010**, *26*, 10147−10157.
(36) Eggenhuisen, T. M.; Prieto, G.; Talsma, H.; de Jong, K. P.; de Jongh, P. E. *J. Phys. Chem. C* **2012**, *116*, 23383−23393.
(37) Kruk, M.; Antochshuk, V.; Matos, J. R.; Mercuri, L. P.; Jaroniec, M. *J. Am. Chem. Soc.* **2002**, *124*, 768−769.
(38) Kim, T.-W.; Ryoo, R.; Kruk, M.; Gierszal, K. P.; Jaroniec, M.; Kamiya, S.; Terasaki, O. *J. Phys. Chem. B* **2004**, *108*, 11480−11489.
(39) Friedrich, H.; de Jongh, P. E.; Verkleij, A. J.; de Jong, K. P. *Chem. Rev.* **2009**, *109*, 1613−1629.
(40) Gommes, C. J.; Friedrich, H.; Wolters, M.; de Jongh, P. E.; de Jong, K. P. *Chem. Mater.* **2009**, *21*, 1311−1317.
(41) Haenel, M. W.; Oevers, S.; Angermund, K.; Kaska, W. C.; Fan, H. J.; Hall, M. B. *Angew. Chem.* **2001**, *113*, 3708−3712.
(42) Liu, Y.; Wang, Y.; Lu, J.; Pinon, V.; Weck, M. *J. Am. Chem. Soc.* **2011**, *133*, 14260−14263.
(43) Goyal, P.; Zheng, X.; Weck, M. *Adv. Synth. Catal.* **2008**, *350*, 1816−1822.
(44) Aerts, S.; Weyten, H.; Buekenhoudt, A.; Gevers, L. E. M.; Vankelecomb, I. F. J.; Jacobsb, P. A. *Chem. Commun.* **2004**, 710−711.